Buildup dynamics of transmission resonances in superlattices

Roberto Romo*
Facultad de Ciencias, Universidad Autónoma de Baja California, Apartado Postal 1880, 22800 Ensenada, Baja California, México
(Received 20 March 2002; revised manuscript received 15 July 2002; published 19 December 2002)

A closed analytical expression for the time-dependent probability density of transmitted particles in superlattices is derived from a formal solution of the time-dependent Schrödinger equation. Such an expression consists of Breit-Wigner type resonance terms and interference contributions with explicit time dependence, which is applied to different superlattices to describe step-by-step how the transmission resonances are constructed as a function of time. In particular, it is found that for incidence at a resonance of position ε_n and width Γ_n, the buildup of the transmission peaks is governed by a simple exponential law $\mathcal{T}_n(\varepsilon_n,t)=T_n^{\mathrm{peak}}[1-\exp(-\Gamma_n t/2\hbar)]^2$, where $\mathcal{T}_n(\varepsilon_n,t)$ is the probability density at the right edge of the superlattice and T_n^{peak} the height of the corresponding transmission peak. We show that our results are valid for periodic superlattices as well as for asymmetrical or even disordered potential profiles.

DOI: 10.1103/PhysRevB.66.245311 PACS number(s): 73.40.Gk, 73.21.Cd

I. INTRODUCTION

The investigation of resonant tunneling in finite superlattices (SL's) has been a field of intense research in the last two decades. These man-made quantum structures have attracted a great deal of interest not only for the possibility of electronic device application,[1] but also for the exploration of a wide variety of transport phenomena both in double and multibarrier systems.[2–6]

In the general study of resonant tunneling, the transmission coefficient has been an important quantity since it provides most of the relevant information of the transport process in SL's, and is characterized by a series of resonance peaks at specific incidence energies. The properties of these transmission resonances and their implications on the electronic transport in semiconductor heterostructures have been extensively studied using solutions of the time-independent Schrödinger equation (TISE),[7–10] which describe physical situations where the stationary regime has already been established. The need of studies of resonant tunneling also with solutions of the time-dependent Schrödinger equation (TDSE) has been widely recognized.[3,6,11] The interest on the study of the transient regime lies in part on the fact that the earliest tunneling events, which have important implications on the speed of resonant tunneling devices, occur within this time domain. Here we address the issue of how the transmission resonances are formed as well as the duration of the corresponding transient.

In the present work we use a dynamical approach[11] to describe step-by-step the time evolution of the buildup of the transmission resonances, starting from the situation in which the SL is initially empty. The initial condition used here is visualized as a shutter placed at the left edge of the system (see sketch in Fig. 1), which for $t<0$ stops incident waves coming from the left, and at $t=0$ the shutter is suddenly removed enabling the incoming wave to interact with the SL potential. For this setup, explicit analytic solutions of the TDSE can be obtained. An interesting feature of this method is that allows us to analyze in a natural way the transition from the transient to the well known stationary regime. This approach is a generalization to tunneling problems, of the free quantum shutter setup that predicted the phenomenon of diffraction in time[12] in 1952, which has been recently verified experimentally.[13] We apply here this formalism to finite SL's to study the buildup dynamics of the transmission resonances and to estimate the time required for the formation of each of the transmission peaks of the SL miniband for a wide range of potential profile parameters; we find that they follow a simple exponential buildup law whose transient time constant can be written explicitly in terms of the resonance width.

The paper is organized as follows. In Sec. II we make a brief presentation of the formalism, which is discussed in more detail in Ref. 11 in which it was recently introduced. In Sec. III we derive an expression for the probability density valid to describe the tunneling dynamics around a miniband. In Sec. IV we apply the derived expression to study the buildup of the transmission resonances for different SL's. Also in that section, we use the link with the transmission coefficient to analyze the duration of the transient and establish the buildup law for the transmission peaks. Finally, in Sec. V we present the concluding remarks.

II. THE FORMAL SOLUTION

In this paper we use a dynamical approach developed by García-Calderón,[11] that deals with the analytic solution of the TDSE

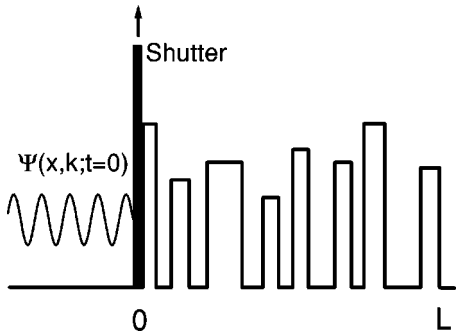

FIG. 1. Shutter problem for a finite SL. The incoming plane wave at $t=0$ exists only at the left of the SL, and is instantaneously released by the sudden removal of the shutter at $t=0$, enabling it to interact with the potential. Note that the shutter is a device that aids in visualization of the initial condition and hence it does not appear as a part of the potential in the Hamiltonian.

$$\left(i\hbar \frac{\partial}{\partial t} - H \right) \Psi = 0, \tag{1}$$

for finite range potentials $V(x)$ of arbitrary shape that vanishes outside the region $0 \leqslant x \leqslant L$. The initial condition used here consists of cutoff plane waves confined to the left of the SL by a reflecting shutter placed at the left edge of the structure, at $x=0$, and is represented by

$$\Psi(x,k;t=0) = \begin{cases} e^{ikx} - e^{-ikx}, & \infty < x \leqslant 0, \\ 0, & x > 0. \end{cases} \tag{2}$$

The onset of tunneling is chosen at t=0 and before this time our noninvasive initial state exists only at the left of the structure, hence the SL is initially empty. Once the shutter is suddenly removed at $t=0$, the initial wave is enabled to interact with the potential giving rise to the transmission through the SL system. For the above initial condition, the solution along the internal region reads[11]

$$\Psi(x,k;t) = \phi(x,k) M[y(k,t)] - \phi^*(x,k) M[y(-k,t)] - \sum_{n=-\infty}^{\infty} \rho_n(x,k) M[y(k_n,t)], \tag{3}$$

where the index n runs over the complex poles k_n of the outgoing Green's function of the system,[11] distributed in the third and fourth quadrants in the complex k plane. The function $\phi(x,k)$ stands for the stationary solution.

The coefficients of the sum are given by

$$\rho_n(x,k) = 2ik \frac{u_n(0) u_n(x)}{k^2 - k_n^2}. \tag{4}$$

To compute these coefficients we basically need to calculate the complex poles k_n and the resonant states $u_n(x)$ which are solutions of the time-independent Schrödinger equation with outgoing boundary conditions.[14]

The time dependence of the solution given by Eq. (3) is contained in the Moshinsky functions $M(y)$, defined as,

$$M(y_q) = \frac{1}{2} w(iy_q), \tag{5}$$

where $w(z) = \exp(-z^2) erfc(-iz)$ is the complex error function.[15] The argument y_q depends on the time through the relation

$$y(q,t) = -e^{-i\pi/4} \left(\frac{m}{2\hbar t} \right)^{1/2} \left[\frac{\hbar q}{m} t \right], \tag{6}$$

where q stands for $\pm k$ or $k_{\pm n}$. The formal solution, Eq. (3), involves the contribution of the full resonant spectrum of the system, and can be used to calculate the probability density $|\Psi(E,x;t)|^2$ for $0 \leqslant x \leqslant L$, at any time t and incidence energy E, provided that the relevant set of resonant states $\{u_n\}$ and complex eigenvalues $\{k_n\}$ of the system are known.

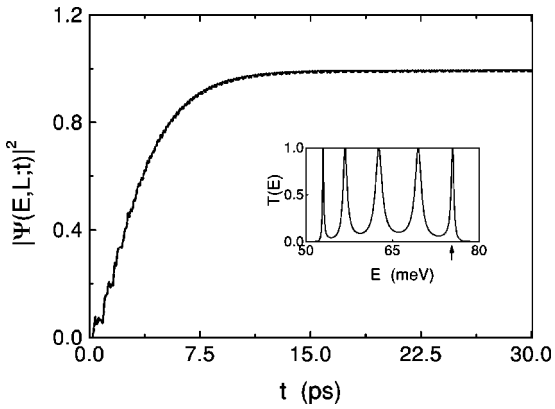

FIG. 2. Comparison of the calculation of $|\Psi|^2$ vs t with Eq. (7) (solid line) and Eq. (3) (dashed line) for a periodic SL of six rectangular barriers with parameters given in the text. The incidence energy ($E=\varepsilon_5=75.4$ meV) is indicated by the arrow in the corresponding T vs E plot shown in the inset.

III. SINGLE MINIBAND APPROXIMATION

In the present study we are interested in the time-dependent description of the probability density in finite superlattices, in which typically the resonances are distributed in isolated groups called minibands. To obtain a description of time-dependent resonant tunneling around a miniband, one can just evaluate the relevant subset of resonance terms in Eq. (3) corresponding to the resonances of such a miniband, and neglecting the small contribution of far away resonances. Using some analytic properties of the Moshinsky functions, it is possible to derive a simple and reliable formula to describe the time-dependent probability density $|\Psi^N(E,t)|^2$ for incidence energies around a miniband consisting of N resonances. Such a derivation is included in Appendix, and the derived expression for $|\Psi^N(E,t)|^2$ is given by in Eq. (A5). If we ignore the negligible contribution R, the single miniband approximation for Eq. (3) reads

$$|\Psi^N(E,t)|^2 \approx \sum_{n=1}^{N} \mathcal{T}_n(E,t) + \sum_{n<m}^{N} \mathcal{T}_{mn}(E,t), \tag{7}$$

where the resonant terms $\mathcal{T}_n(E,t)$ and the interference contributions $\mathcal{T}_{mn}(E,t)$ are given, respectively, by Eqs. (A6) and (A7).

A considerable simplification of the problem has been accomplished with the derivation of the above formula, note for example that the time dependence (originally contained in the Moshinsky functions) is now expressed in terms of simple functions, see Eqs. (A8) and (A9).

In order to illustrate the accuracy of our approximate formula, Eq. (7), we shall illustrate its reliability with a pair of numerical examples. Our first example is a simple periodic SL of six rectangular barriers of height $V_0=0.3$ eV, and width $b_0=2.5$ nm, with well widths $w_0=6.5$ nm (similar to the parameters used by Pacher[16] *et al.*). In all the examples of this paper we use the effective mass $m=0.067m_e$, where m_e is the mass of the electron. Figure 2 shows the results of the comparison of Eq. (7) (solid line) with Eq. (3) (dashed line) for this sample. The incidence energy was chosen to

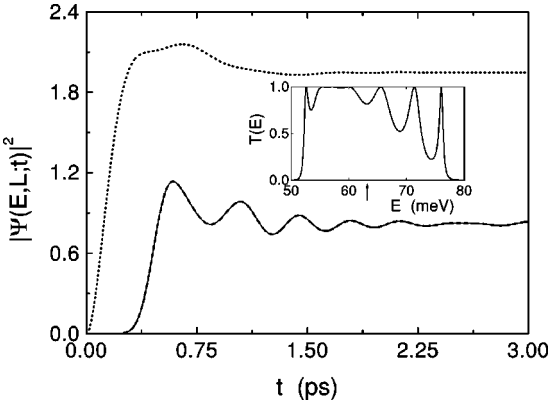

FIG. 3. The same as in Fig. 2 for a SL with strong interference between the resonances of the first miniband. Also in this case the solid and dashed lines are indistinguishable among them. Here, as indicated by the arrow in the inset, the incidence energy was chosen approximately in the center of the miniband ($E=63.31$ meV). If the interference terms $\mathcal{T}_{mn}(E,t)$ are ignored, a very bad description is obtained (dotted line), note that the corresponding curve lies well above unity.

coincide with one of the resonances ($E=\varepsilon_5$), see arrow in inset of Fig. 2. We can appreciate that the calculation with Eq. (7) successfully reproduces the predictions of the formal solution, Eq. (3), since both curves are almost indistinguishable among them. This result supports our conjecture that R has in Eq. (A5) a negligible small contribution.

In order to emphasize on the importance of the interference terms $\mathcal{T}_{mn}(E,t)$, we choose as a second example a SL with a strong interaction between the resonances belonging to a miniband. For this purpose, the ''SL with antireflection coating'' studied by Pacher and co-workers[16] is an appropriate example in view of the extremely high interference exhibited in the transmission coefficient. This SL is the eight-barrier structure that consists of the periodic SL of six barriers of the previous example, with two additional ''half barriers'' of width $b_1=b_8=1.25$ nm and two additional wells of width $w_1=w_7=6.5$ nm. The results of the comparison of Eq. (3) and Eq. (7) are depicted in Fig. 3. As in the previous case, the insets shows the corresponding transmission coefficient versus energy plot around the first miniband, and the arrow indicates the incidence energy, off-resonance in this case ($E=63.31$ meV). We can appreciate that even in this case of high interference among the resonances of the miniband, the calculation with Eq. (7) (solid line) successfully reproduces the predictions of the formal solution, Eq. (3) (dashed line). Also in this case of intense interference and off-resonance incidence, R has a negligible contribution, implying that Eq. (7) is an excellent approximation even for SL's with overlapping resonances.

Note also that the plots of $|\Psi|^2$ vs t, calculated from our formula (7) leads to the correct asymptotic values at long times. In fact, we can appreciate in Figs. 2 and 3 that it tends to 1.0 and 0.818, respectively, which are exactly the values of the transmission coefficient for the chosen incidence energies, fulfilling the requirement $|\Psi(E,L,t\rightarrow\infty)|^2=|\phi(E,L)|^2$.[11]

In contrast to the neglecting contribution of R, the interference terms $\mathcal{T}_{mn}(E,t)$ are very important. The contribution of the latter may, in some cases, be of the order of or even larger than the contribution of the resonant terms $\mathcal{T}_n(E,t)$. To illustrate the above we have included in Fig. 3 the calculations of $|\Psi|^2$ ignoring the interference contributions $\mathcal{T}_{mn}(E,t)$; that is, using the ''incomplete'' formula $f(E,t)=\sum_{n=1}^{N}\mathcal{T}_n(E,t)$, in which the interference contributions are absent (dotted line). It is clearly evident that if we ignore the interference contributions, a very bad description may be obtained, not only in the transient regime but also in the asymptotic limit of long times. Therefore, we stress out that in our dynamical description of resonant tunneling around a miniband, the contribution of the interference terms $\mathcal{T}_{mn}(E,t)$ is essential.

IV. BUILDUP OF TRANSMISSION RESONANCES

In this section we shall study step-by-step the process of construction of the transmission resonances. In order to perform this task, we apply the time-dependent expression given by Eq. (7) to SL's with diverse shape parameters that exhibit different distribution of resonances.

A. Examples

1. Periodic SL

We start our discussion with the simplest of the SL's, the periodic structure. Let us consider the system consisting on five rectangular barriers with heights $V_0=0.2$ eV and widths $b_0=5.0$ nm and well widths $w_0=5.0$ nm. Figure 4 shows a series of plots of $|\Psi^N(E,L;t)|^2$ vs E at different fixed times, calculated using Eq. (7) with $N=4$ (solid line). The transmission coefficient $T(E)$, calculated by the standard method of the transfer matrix approach is included for comparison (dotted line), which, in the absence of an external field is given by

$$T(E)=1/|M_{22}|^2, \tag{8}$$

where M_{22} is an element of the transfer matrix $\mathbf{M}$ of the system.

In the snapshots depicted in Figs. 4(b)–4(e) we can appreciate the ''birth'' of the transmission resonances and their subsequent evolution towards the well known stationary regime. At the very beginning of the tunneling process, the plot of $|\Psi^N(E,L;t)|^2$ vs E appears as a smooth curve with no peaks, see Fig. 4(b); that is, no evidence of the resonances have appeared at this early stage. However, as time elapses some peaks in the curve gradually begin to appear as we can see in Figs. 4(c)–4(e). The height of such resonance peaks increases at different rates towards their corresponding asymptotic values. In Fig. 4(e), where we used $t=80$ ps, we can see that the predicted values by Eq. (7) perfectly reproduce the transmission coefficient at large enough times, showing that the stationary situation is reached in the appropriate asymptotic limit. Notice that the buildup of the peaks is faster for the wider resonances ($n=2$ and 3), and slower for the thinner ones ($n=1$ and 4). As we shall see in the

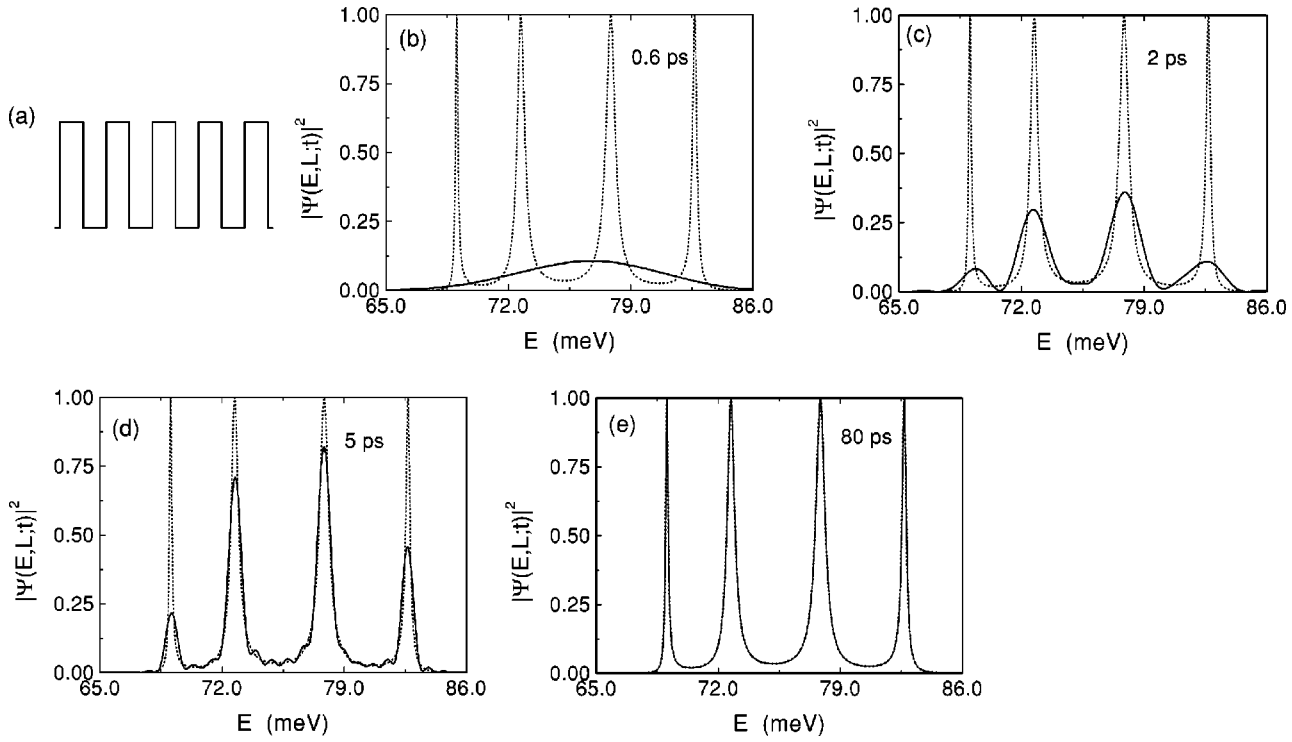

FIG. 4. Snapshots of the time-dependent probability density for the periodic SL of five barriers (a), with equal heights $V_0=0.2$ eV, widths $b_0=5.0$ nm, and well widths $w_0=5.0$ nm. The values of $|\Psi|^2$ vs E are calculated using Eq. (7) (solid lines) at different fixed times: (b) $t=0.6$ ps, (c) $t=2.0$ ps, (d) $t=5.0$ ps, (e) $t=80.0$ ps. The transmission coefficient is also included for comparison (dotted lines).

following examples, this behavior is also observed in SL's with other arbitrarily chosen potential parameters.

2. SL with overlapping resonances

In the above example we described a situation in which the neighboring resonance levels of the miniband are almost equally spaced, having a relatively small interference between them. However, one of the advantages of Eq. (7) is that it can describe successfully situations in which the resonances have a strong interference between them. Pairs of overlapping resonances (doublets) can be obtained for example from symmetric potentials with a relatively wide central barrier (or central well, if the number of barriers is even), or with a relatively thin central barrier (or well). As an example, let us consider a SL consisting of six rectangular barriers with equal heights $V_0=0.1$ eV and widths $b_0=4.0$ nm, a central well of width $w_3=5.0$ nm, narrower than the rest, which have the common width $w_n=7.0$ nm ($n=1$, 2, 4, 5). The potential profile is sketched in Fig. 5(a)

As can be appreciated in Figs. 5(b)–5(e), the transmission coefficient around the first miniband consists of two pairs of overlapping peaks and a single isolated peak (dotted lines). The behavior of $|\Psi^N(E,L;t)|^2$ vs E predicted by Eq. (7) (with $N=5$), for different fixed times are shown in a series of snapshots, see solid line in Figs. 5(b)–5(e). As is clearly evident, also in this SL an excellent agreement with the stationary solution is obtained for long times. Note that, as in the previous example, the buildup of the transmission peaks occurs in such a way that it is faster for the wider and slower for the thinner resonances.

3. Irregular SL

As a final example, let us now consider a totally irregular structure whose potential profile is sketched in Fig. 6(a), which is an ''intentionally disordered'' SL of eight barriers with the following potential parameters: barrier heights $\{V_n\}=\{0.25,0.40,0.30,0.50,0.26,0.30,0.35,0.23\}$ (eV); barrier widths $\{b_n\}=\{2.5,1.5,3.8,1.0,3.0,3.2,2.0,2.7\}$ (nm); and well widths $\{w_n\}=\{5.0,5.5,5.1,4.8,5.2,4.5,5.0\}$ (nm). Snapshots of the behavior of $|\Psi^N(E,L;t)|^2$ vs E are depicted in Figs. 6(b)–6(e) for different fixed times. As in the two previous figures, here the continuous line corresponds to the values of $|\Psi^N(E,L;t)|^2$ vs E calculated from the approximate expression given by Eq. (7) with $N=7$, and the transmission coefficient $T(E)$, calculated from Eq. (8), is represented by the dotted line. As expected, the observed behavior is more complex than in the previous two examples. In contrast with the cases of Figs. 4 and 5 of unity transmission peaks, for this irregular potential the transmittance is very low for most of the resonances (for example the fifth peak is so small and wide that is difficult to see it in the graph). However, despite of this complexity, once again Eq. (7) gives an excellent description, and perfectly reproduces the transmission coefficient at long enough times as can be appreciated in Fig. 6(e).

Notice that also in this case the wider resonances are the first established around the asymptotic value (as observed in the two previous examples). This leads to a natural question: What is the duration of the transient for each of the transmission resonances according to their corresponding widths

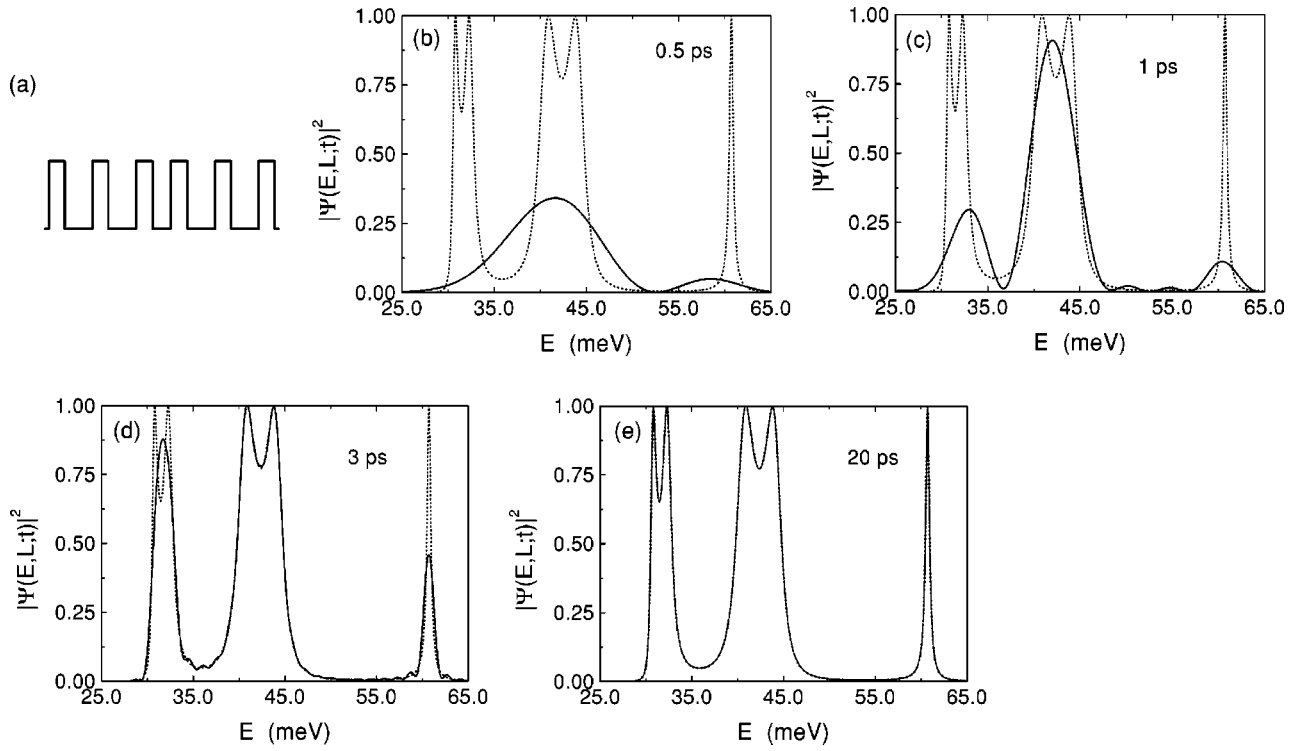

FIG. 5. The same as in the previous figure for a symmetrical SL with central well narrower that the rest (a) (see parameters in the text). The plots of $|\Psi|^2$ vs E were calculated at the times: (b) $t=0.5$ ps, (c) $t=1.0$ ps, (d) $t=3.0$ ps, (e) $t=20.0$ ps (solid lines). As expected, we see that a perfect fit with the transmission coefficient is achieved at long enough times.

Γ_n? We shall discuss this point at the end of this section, and show that the buildup of the transmission resonances follows a simple exponential law whose transient time constant depends on the width Γ_n of the resonances. In order to perform this task, we need to explore analytically the link of the quantity $|\Psi^N(E,t)|^2$ with the transmission coefficient $T(E)$. This is the purpose of the next subsection.

B. Transmission coefficient

In the above numerical examples, it is clearly evident that the approximate expression for $|\Psi^N(E,t)|^2$ evolves towards the correct asymptotic limit (the transmission coefficient), despite the fact that it involves only a finite number of resonance contributions. Although in the general case (in which the full resonant spectrum of the system is considered) García-Calderón and Rubio[11] have already demonstrated that $|\Psi(L,k;t)|\rightarrow|t(k)|$ as $t\rightarrow\infty$, where $t(k)$ is the transmission amplitude, it is instructive to explore here the analytic connection of our approximate quantity $|\Psi^N(E,t)|^2$ with an explicit analytic expression of the transmission coefficient $T(E)$. Using the definition of the partial decay widths Γ_n^0 and Γ_n^L, we shall obtain an expression for $|\Psi^N(E,t)|^2$ that will be used in the next subsection to analyze the duration of the buildup of each of the transmission peaks.

The partial widths are given by[10]

$$\Gamma_n^0=\frac{\hbar^2 a_n}{mI_n}|u_n(0)|^2 \tag{9}$$

and

$$\Gamma_n^L=\frac{\hbar^2 a_n}{mI_n}|u_n(L)|^2. \tag{10}$$

Here a_n is the real part of k_n and $I_n=\int_0^L|u_n(x)|^2dx\approx 1$, and the sum of the partial widths is equal to the total width $\Gamma_n=\Gamma_n^0+\Gamma_n^L$.

The above quantities can be used in the expressions of $\mathcal{T}_n(E,t)$ and $\mathcal{T}_{mn}(E,t)$ (derived in the Appendix) to obtain new explicit formulas that allow us to explore analytically the link of $|\Psi^N(E,t)|^2$ with the transmission coefficient $T(E)$. From Eqs. (4), (9), and (10), we obtain after a simple algebra a Breit-Wigner type expression for $|\rho_n(L,k)|^2$ in terms of Γ_n^0 and Γ_n^L. Using such an expression in Eq. (A6), the quantity $\mathcal{T}_n(E,t)$ can be rewritten as

$$\mathcal{T}_n(E,t)=T_n(E)\chi_n(E,t), \tag{11}$$

where

$$T_n(E)=C_n\left[\frac{\Gamma_n^0\Gamma_n^L}{\hat{\omega}_n^2+(\Gamma_n/2)^2}\right]. \tag{12}$$

Notice that, although the time dependence in Eq. (11) appears only in the factor χ_n, both T_n and χ_n have in common the energy E and hence they are still coupled. This coupling is important in the transient regime and gradually disappears as the solution evolves towards the stationary situation. The

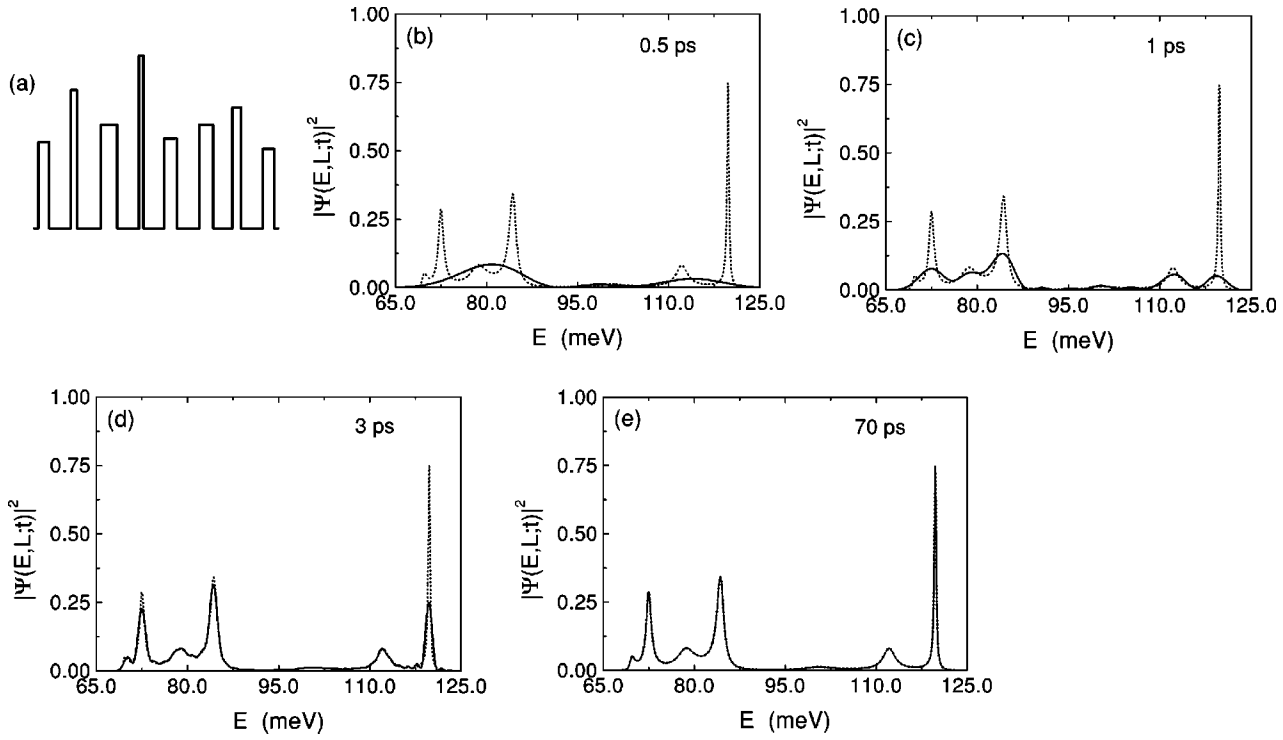

FIG. 6. The same as in the two previous figures for a SL with an irregular potential profile (a) with parameters given in the text. The plots of $|\Psi|^2$ vs E were calculated at the times: (b) $t=0.5$ ps, (c) $t=1.0$ ps, (d) $t=2.0$ ps, (e) $t=70.0$ ps. Even for this highly irregular potential, a perfect fit with the transmission coefficient is achieved at long times.

above is obvious from the fact that $\chi_n(E,t)\rightarrow 1$ when $t\rightarrow\infty$ as can be easily verified.

The interference terms $\mathcal{T}_{mn}(E,t)$ can also be expressed in terms of the partial decay widths Γ_n^0 and Γ_n^L. After using Eqs. (4), (9), and (10) in Eq. (A7), the following analytic expression is obtained:

$$\mathcal{T}_{mn}(E,t)=2C_{mn}(\Gamma_m^0\Gamma_m^L\Gamma_n^0\Gamma_n^L)^{1/2}\times\mathrm{Re}\left[\frac{\exp[i(\phi_{mn})]\xi_{mn}(E,t)}{(\hat{\omega}_m+i\Gamma_m/2)(\hat{\omega}_n-i\Gamma_n/2)}\right], \quad (13)$$

where $C_n=(k/a_n)^2I_n^2$ and $C_{mn}=(k^2/a_ma_n)I_mI_n$, $\phi_{mn}\equiv[\phi_m(0)+\phi_m(L)-\phi_n(0)-\phi_n(L)]$, the ϕ_n's being the phases of the resonant states, i.e., $u_n(x)=|u_n(x)|\exp[i\phi_n(x)]$.

Also in the terms $\mathcal{T}_{mn}(E,t)$, the time dependent factor $\xi_{mn}(E,t)$ is coupled to the rest of the expression through the energy E. It is straightforward to see that if we let $t\rightarrow\infty$, we have $\xi_{mn}(E,t)\rightarrow 1$ and as a consequence, the asymptotic expression of Eq. (7) coincides exactly with the analytic expression of the transmission coefficient $T(E)$ derived in Ref. 10 for multibarrier resonant structures.

C. Duration of the transient

In the examples of the previous sections, we noticed that the wider resonance peaks rise up to the level of the stationary value faster than the thiner ones. The purpose of this section is give an estimate of the duration of this transient in terms of the width Γ_n of the resonances.

For incidence at one of the resonances, say $E=\varepsilon_n$, we have: $\hat{\omega}_n=0$, $k\approx a_n$, and hence $\mathcal{T}_n(E,t)$ adopts a very simple form, namely,

$$\mathcal{T}_n(\varepsilon_n,t)=T_n^{\mathrm{peak}}[1-\exp(-t/2\tau_n)]^2, \quad (14)$$

where

$$T_n^{\mathrm{peak}}=\frac{4\Gamma_n^0\Gamma_n^L}{(\Gamma_n^0+\Gamma_n^L)^2} \quad (15)$$

is the maximum of the transmission coefficient at the nth resonance energy, and $\tau_n=\hbar/\Gamma_n$ is the corresponding lifetime. Note that in general, for asymmetric potentials we have $\Gamma_n^0\neq\Gamma_n^L$ and hence T_n^{peak} may have values below unity (this is the case of the irregular structure whose transmission coefficient is plotted in Fig. 6). It is clear from Eq. (15) that $T_n^{\mathrm{peak}}=1$ only occurs in the case in which the partial decay widths coincide, $\Gamma_n^0=\Gamma_n^L=\Gamma_n/2$. Although the under-unity transmission is easily explained here with Eq. (15), it is important to mention that the situation is more subtle when the interference between neighboring resonances is very strong. In this special situation, under-unity transmission peaks have been observed even in symmetrical structures.[9]

Equation (14) tells us that the buildup of each of the transmission peaks follows an exponential law in which the transient time constant τ_n is twice the value of the lifetime of the

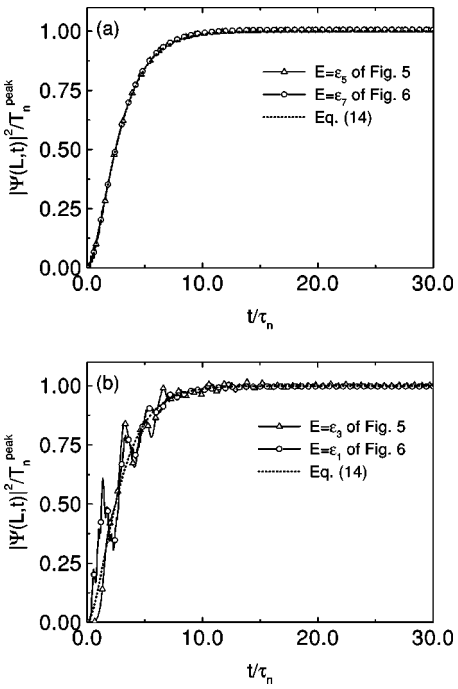

FIG. 7. Plots of $|\Psi|^2$ normalized to T^{peak} vs time t normalized to the corresponding lifetime $\tau_n=\hbar/\Gamma_n$, for incidence at (a) isolated and (b) overlapping resonances. In (a), the curve with hollow triangles corresponds to $E=\varepsilon_5$ for the symmetric SL of Fig. 5, and hollow circles to $E=\varepsilon_7$ for the irregular SL of Fig. 6. The curves in (b) with hollow triangles and hollow circles correspond, respectively, to $E=\varepsilon_3$ and $E=\varepsilon_1$ for the same two SL's. Also shown is the calculation made by Eq. (14) (dotted line), which gives a good description for the different cases depicted here.

resonance. This implies, in particular, that the wider resonances build up faster than the thinner resonances, a result that is consistent with the numerical examples presented in the previous sections.

An interesting result is that Eq. (14) predicts the same buildup law for any of the resonances of the miniband, and makes no distinction between different systems: it applies to the transmission resonances of both periodic SL's (for which $T_n^{\text{peak}}=1$) and asymmetrical or disordered SL's (for which typically $T_n^{\text{peak}}\leqslant 1$). This kind of ''universality'' is illustrated in Fig. 7, in which we have (arbitrarily) chosen some of the resonances of two SL's with quite different potential profiles. In Fig. 7(a), using Eq. (7), we plot $|\Psi^N|^2/T_n^{\text{peak}}$ vs τ, where $\tau\equiv t/\tau_n$, for the SL's of the second and third examples of Sec. IV, where the incidence energy was chosen to coincide with the position of their sharper resonances, which, by simple inspection of Figs. 5 and 6, are $E=\varepsilon_5$ in the former and $E=\varepsilon_7$ in the latter. As we can see in Fig. 7(a), a perfect fit is obtained with the exponential curve given by Eq. (14) despite the fact that we are considering different resonances of different SL's.

Let us consider now a couple of cases with incidence at wider and overlapping resonances. In view of interference effects between neighboring resonances, some ''noise'' is expected in this case. This situation is illustrated in Fig. 7(b), in which, for the same two SL's used in Fig. 7(a), we used $E=\varepsilon_3$ in the former (one of the peaks of the second doublet of Fig. 5) and $E=\varepsilon_1$ in the latter (see the first small peak in Fig. 6). We see in Fig. 7(b) that the corresponding plots also fit to the same exponential curve, except for the small oscillations, which, as mentioned above, is the noise produced by the influence of the interference with neighboring resonances. It is important to emphasize that Eq. (14) is a single resonance approximation which does not include interference contributions, hence the imperfect fit observed in Fig. 7(b) is not surprising; in fact, the amplitude of the oscillations may increase for resonances with stronger overlap. However, despite this noise the fitting is still good, and even the results shown in Fig. 7(b) are good enough to establish that the buildup of the transmission peaks is roughly governed by the exponential formula given by Eq. (14).

Note the resemblance of the derived buildup law, Eq. (14), with the buildup law of a charging-up capacitor in a RC circuit, $Q(t)=Q[1-\exp(-t/\tau_{\text{RC}})]$, where τ_{RC} is the transient time constant. In our quantum system, according to Eq. (14), the transient time constant that characterizes the buildup of the transmission resonances is twice the value of the lifetime of the resonance, namely,

$$\tau_n^{\text{res}}\approx 2\,\tau_n=2\hbar/\Gamma_n\,. \tag{16}$$

The above is a relevant time scale that characterizes the duration of the transient, and can be easily calculated for any of the resonances of the miniband provided the corresponding width Γ_n is known. It is interesting that a transient time constant of also twice the value of the natural lifetime was found by Pastawski some years ago using a different approach.[17] He studied the time-dependent resonant tunneling in the presence of dephasing processes using a formalism based on a modified Landauer-Büttiker picture. Although our description is based on a more idealized model, it gives a clear description of time-dependent resonant tunneling not only in the regime of short times, it also succesfully describes the transition from the transient to the stationary regime.

To complete our discussion, we end this section illustrating the time evolution of the integrated probability density at $x=L$,

$$I_L(t)=\int_{E_1}^{E_2}|\Psi(E,L;t)|^2dE. \tag{17}$$

For the case of the periodic SL considered in Fig. 4, we show in Fig. 8 a plot of $I_L(t)/I_0$ vs t, where $I_0=\int_{E_1}^{E_2}T(E)dE$, with the integration performed along an energy interval $[E_1,E_2]$ that extends around the first miniband (in the present calculation, $E_1=65.0$ meV and $E_2=86.0$ meV, as in Fig. 4). As can be seen, when $t\to\infty$ the value of the integral $I_L(t)$ tends smoothly to the correct asymptotic limit, I_0. The features exhibited by $I_L(t)$ before it reaches the asymptotic value are the effects of the changes in the shape of the $|\Psi|^2$ vs E curves occurring during the transient regime. As seen in the snapshots of Fig. 4, dramatic variations of the shape of the $|\Psi|^2$ vs E plots are observed at the different stages, mainly due to the birth of the resonance peaks at early times, and the

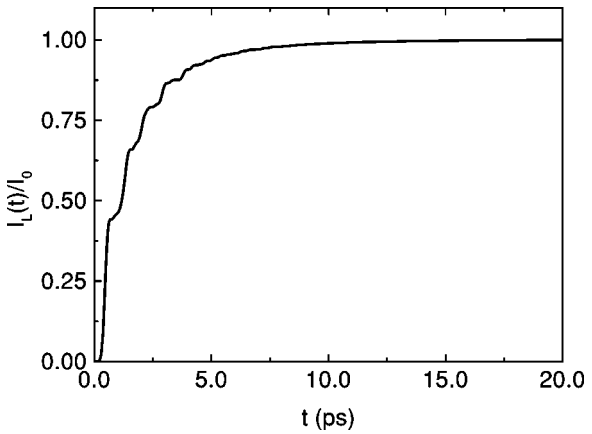

FIG. 8. Plot of $I_L(t)/I_0$ vs t for the periodic case considered in Fig. 4. The limits of the integrals were chosen also as in Fig. 4, i.e., $E_1=65.0$ meV and $E_2=86.0$ meV.

relatively fast increase of their heights (and simultaneous decrease of their widths). As a consequence of these variations, during this transient the integrated probability density exhibits the steplike fluctuations observed in Fig. 8. A qualitatively similar behavior (not shown here) is observed in the $I_L(t)/I_0$ vs t plots for the SL with overlapping resonances of Fig. 5 and the irregular SL of Fig. 6.

V. CONCLUDING REMARKS

A time-dependent description of resonant tunneling in SL's around a miniband has been accomplished. Starting from the formal solution of the TDSE for cutoff initial waves incident on one side of the potential, a closed analytic expression for the probability density at the right edge of the SL has been derived. It consists of a finite number N of Breit-Wigner-type resonance terms plus interference contributions with explicit time dependence. This approximate formula is applied to superlattices with quite different distribution of resonances and an excellent description is obtained if the number N is taken equal to the number of resonances of the miniband. It also applies to superlattices with potential parameters such that the resonance levels are closely spaced presenting significant interference among them. The interference effects due to the multiple interaction between the N resonances of the miniband and the incidence energy give rise to oscillatory contributions with frequencies $\omega_n=|E-\varepsilon_n|/\hbar$ and $\omega_{mn}=|\varepsilon_m-\varepsilon_n|/\hbar$. As discussed elsewhere, these frequencies play relevant role on the dynamics of the tunneling process, in particular they can be tuned by a proper choice of the incidence energy in order to enhance the tunneling probability of the earliest transmitted carriers.[18] Within the framework of this dynamical approach, we study the way in which the transmission resonances are formed as a function of time, and show that they are governed by a simple exponential buildup law $\mathcal{T}_n(\varepsilon_n,t)=T_n^{\mathrm{peak}}[1-\exp(-t/\tau_n^{\mathrm{res}})]^2$, whose transient time constant τ_n^{res} is twice the value of the lifetime of the resonant state $\tau_n^{\mathrm{res}}\approx 2\tau_n=2\hbar/\Gamma_n$.

As a final remark, it is worth to mention that an important problem in this context has been the investigation of the relevant time scales for the passage of electrons across the SL. A recent work on the subject was made by Pereyra[19] using a stationary approach valid for finite periodic SL's, in which the *phase time* was analyzed in a wide range of energies. We believe that this problem also deserves a time-dependent analysis in order to obtain information of the earliest tunneling events that occur in the transient regime. One of the features of the approach used here is that leads to analytic solutions of the TDSE that allow to analyze the transition from the transient to the stationary regime, having the possibility to explore not only the dynamics of the emission at $x=L$ of the earliest transmitted particles, but also its relation to the buildup dynamics inside the SL. Moreover, our approach is valid not only for periodic SL's, it also applies to irregular (disordered) potentials and consequently it may allows us to observe the localization phenomena in a time-dependent picture. This investigation is considered for future work.

ACKNOWLEDGMENTS

I am indebted to Jorge Villavicencio for many useful discussions and suggestions. Discussions with Gastón García-Calderón are also acknowledged. This work is supported financially by Conacyt, México, through Contract No. 431100-5-32082E.

APPENDIX

The approximation to Eq. (3) for one miniband consisting on N resonances is

$$\Psi\approx\Psi^N=\phi^N M[y(k,t)]-\phi^{*N}M[y(-k,t)]-\sum_{n=1}^{N}\{\rho_n M[y(k_n,t)]+\rho_{-n}M[y(k_{-n},t)]\}. \quad \text{(A1)}$$

Here ϕ^N denotes the miniband approximation of the stationary solution $\phi(x,k)$, which is given by[10]

$$\phi(x,k)\approx\phi^N(x,k)=2ik\sum_{n=1}^{N}\frac{u_n(0)u_n(x)}{k^2-k_n^2}. \quad \text{(A2)}$$

The M functions involved in Eq. (A1) exhibit different behavior as functions of time depending on the value of the phase of its complex argument $y\equiv|y|\exp(i\theta)$. When $-\pi/2<\theta<\pi/2$, $M(y)$ is a decreasing function of time. In fact, at long times it can be represented in terms of inverse powers of t by the series[11] $M(y)\sim(1/2)[1/(\pi^{1/2}y)-1/(\pi^{1/2}y^3)+\cdots]$. As can be easily verified, only the functions $M[y(q,t)]$ in Eq. (3) with $q=-k$ and $q=k_{-n}$ lie in this category. Therefore, it is expected that, compared with the exponential terms, these functions have a relatively small contribution to the solution.[20]

On the other hand, it is not difficult to convince oneself that for M's with $q=+k$ and $q=+k_n$ the inequality $-\pi/2<\theta<\pi/2$ is not fulfilled, and hence the above arguments

does not apply to both $M[y(k,t)]$ and $M[y(k_n,t)]$. Fortunately, they can be related with the other M functions by the symmetry relation[11]

$$M(y)=e^{y^2}-M(-y), \tag{A3}$$

by noting that $-y(q,t)=y(-q,t)$. By feeding Eq. (A3) and Eq. (A2) into Eq. (A1), the solution at the right edge ($x=L$) of the SL can be rewritten in the form

$$\Psi^N(k,t)=\sum_{n=1}^{N}\rho_n(L,k)[e^{[y(k,t)]^2}-e^{[y(k_n,t)]^2}]+\Delta(L,k;t), \tag{A4}$$

where $\Delta(L,k;t)$ accounts for all the terms containing M functions of the form $M[y(-k,t)]$ and $M[y(k_{-n},t)]$, which, as mentioned above, are decreasing functions of t with negligible contribution.

A useful analytic expression for the probability density at $x=L$ can be easily calculated from Eq. (A4). After a straightforward algebra it reads

$$|\Psi^N(E,t)|^2=\sum_{n=1}^{N}\mathcal{T}_n(E,t)+\sum_{n<m}^{N}\mathcal{T}_{mn}(E,t)+R, \tag{A5}$$

where the term R involves the negligible contributions coming from the term $\Delta(L,k;t)$. $\mathcal{T}_n(E,t)$ and the interference terms $\mathcal{T}_{mn}(E,t)$ are given, respectively, by

$$\mathcal{T}_n(E,t)=|\rho_n|^2\chi_n(E,t) \tag{A6}$$

and

$$\mathcal{T}_{mn}(E,t)=2\,\mathrm{Re}\{\rho_m\rho_n^*\xi_{mn}(E,t)\}, \tag{A7}$$

$E=\hbar^2k^2/2m$ being the incidence energy. Notice that the time dependence is now contained in the functions χ_n and ξ_{mn}, which have the following closed analytic expressions

$$\chi_n(E,t)=1-2\cos(\hat{\omega}_n t)e^{-\Gamma_n t/2\hbar}+e^{-\Gamma_n t/\hbar}, \tag{A8}$$

$$\xi_{mn}(E,t)=[1-e^{i\hat{\omega}_m t-\Gamma_m t/2\hbar}-e^{-i\hat{\omega}_n t-\Gamma_n t/2\hbar}+e^{-i\hat{\omega}_{mn}t-(\Gamma_m+\Gamma_n)t/2\hbar}]. \tag{A9}$$

We have defined here the quantities $\hat{\omega}_n\equiv(E-\varepsilon_n)/\hbar$, and $\hat{\omega}_{mn}\equiv(\varepsilon_m-\varepsilon_n)/\hbar$, where ε_n is the position of the nth resonance and Γ_n the corresponding width. Their absolute values correspond to different oscillation frequencies $\omega_n=|\hat{\omega}_n|$ and $\omega_{mn}=|\hat{\omega}_{mn}|$ which arise as a result of the multiple interaction between resonant states, and the incidence energy.

*Electronic mail: romo@uabc.mx

[1] *Nanotechnology: Research and Perspectives*, edited by B. C. Crandall and J. Lewis (MIT Press, Cambridge, London, 1992); *Applications of Quantum Wells and Superlattices*, edited by E. E. Médez and K. von Klitzing (Plenum, New York and London, 1987).

[2] L. Pavesi and F. K. Reinhart, Phys. Rev. B **42**, 11 362 (1990); A. Chomette, B. Deveaud, A. Regreny, and G. Bastard, Phys. Rev. Lett. **57**, 1464 (1986).

[3] T. C. L. G. Sollner, E. R. Brown, W. D. Goodhue, and H. Q. Le, Appl. Phys. Lett. **50**, 332 (1987); M. Tsuchiya, T. Matsusue, and H. Sakaki, Phys. Rev. Lett. **59**, 2356 (1987); H. Yoshimura, J. N. Schulman, and H. Sakaki, Phys. Rev. Lett. **64**, 2422 (1990).

[4] C. Rauch, G. Strasser, K. Unterrainer, E. Gornik, and B. Brill, Appl. Phys. Lett. **70**, 649 (1997).

[5] C. Rauch, G. Strasser, K. Unterrainer, W. Boxleitner, E. Gornik, and A. Wacker, Phys. Rev. Lett. **81**, 3495 (1998).

[6] B. Ricco and M. Y. Azbel, Phys. Rev. B **29**, 1970 (1984).

[7] R. Tsu and L. Esaki, Appl. Phys. Lett. **22**, 562 (1973).

[8] G. Gildenblat, B. Gelmont, and S. Vatania, J. Appl. Phys. **77**, 6327 (1995); C. L. Roy and A. Khan, Phys. Status Solidi B **176**, 101 (1993); X. W. Liu and A. P. Stamp, Phys. Rev. B **47**, 16 605 (1993).

[9] J. Leo and G. A. Toombs, Phys. Rev. B **43**, 9944 (1991); H. Yamamoto, Y. Kanie, and K. Taniguchi, Phys. Status Solidi B **167**, 571 (1991); R. Romo and G. García-Calderón, Phys. Rev. B **49**, 14 016 (1994); Y. S. Joe, D. S. Ikeler, R. M. Cosby, A. M. Satanin, and C. S. Kim, J. Appl. Phys. **88**, 2704 (2000).

[10] G. García-Calderón, R. Romo, and A. Rubio, Phys. Rev. B **47**, 9572 (1993).

[11] G. García-Calderón and A. Rubio, Phys. Rev. A **55**, 3361 (1997).

[12] M. Moshinsky, Phys. Rev. **88**, 625 (1952).

[13] P. Szriftgiser, D. Guéry-Odelin, M. Arndt, and J. Dalibard, Phys. Rev. Lett. **77**, 4 (1996).

[14] The complex eigenvalues k_n can be alternatively calculated as the poles of the transmission amplitude $t(k)$ using an existing relationship between this quantity and the outgoing Green's function of the problem [see Eq. (2) in G. García-Calderón and A. Rubio, Phys. Rev. B **36**, 4462 (1987)]. The eigenfunctions $u_n(x)$ can be obtained by a straightforward calculation using the transfer matrix method adapted to outgoing boundary conditions [R. Romo, Ph.D. thesis, CICESE, México, 1995] and using the corresponding normalization condition [see Eq. (4) in Ref. 10].

[15] *Handbook of Mathematical Functions*, edited by M. Abramowitz and I. A. Stegun (Dover, New York, 1965), p. 297; V. N. Fadeyeva and N. M. Tarent'ev, *Mathematical Tables* (Pergamon, London, 1961).

[16] C. Pacher, C. Rauch, G. Strasser, E. Gornik, F. Elsholz, A. Wacker, G. Kießlish, and E. Schöll, Appl. Phys. Lett. **79**, 1486 (2001).

[17] H. M. Pastawski, Phys. Rev. B **46**, 4053 (1992).

[18] R. Romo, J. Villavicencio, and G. García-Calderón, Phys. Rev. B **66**, 033108 (2002).

[19] P. Pereyra, Phys. Rev. Lett. **84**, 1772 (2000).

[20] Except at very short and very long times, where deviations from the exponential behavior has been observed in the analysis of the Moshinsky functions [G. García-Calderón and A. Rubio, Phys. Rev. A **55**, 3361 (1997)].